Correction and pointer reading recognition of circular pointer meter

OPEN ACCESS
IOP Publishing
Measurement Science and Technology
Meas. Sci. Technol. **34** (2023) 025406 (17pp)
https://doi.org/10.1088/1361-6501/ac9ad4

Correction and pointer reading recognition of circular pointer meter

Dongsheng Ji[1], **Wenbo Zhang**[1], **Qianchuan Zhao**[3] and **Wen Yang**[2,3,*]

[1] School of Computer and Communication, Lanzhou University of Technology, Lanzhou, Gansu Province 620100, People's Republic of China
[2] Xichang Satellite Launch Center, XiChang, Sichuan 615000, People's Republic of China
[3] Center for Intelligent and Networked Systems (CFINS), Department of Automation, Tsinghua University, Beijing 100084, People's Republic of China

E-mail: whutyw@126.com

Received 23 August 2022, revised 4 October 2022
Accepted for publication 17 October 2022
Published 28 November 2022

Abstract

For the meter images collected in an actual environment, there is the possibility of tilt and rotation. This paper presents a method to calibrate the circular pointer-type meter based on YOLOv5s network. The convolutional neural network framework is used to detect the scale value in the meter panel as the key point. The position information and value information of the detected scale value are used to fit the elliptic equation of the position of the scale value with the least square method for perspective correction and rotation correction of the meter, and the corrected meter image is used to obtain the meter pointer reading. This paper proposes the weighted angle method to read the meter reading. After multiple transformations, the accumulated error of the meter image is eliminated. Finally, comparing the pointer detection method of this paper with the traditional pointer detection method, the error of this detection method is smaller; comparing the meter reading results before and after correction, the meter reading error after correction is 50% less than before correction. Comparing the method in this paper with other mainstream methods, it proves the effectiveness of the our method.

Keywords: pointer-type meter, convolutional neural network (CNN), meter correction, angle method, least square method, pointer reading recognition

(Some figures may appear in colour only in the online journal)

1. Introduction

Pointer-type meters have the advantages of a wide range of applications, low environmental impact and high accuracy, so they are used in most plants [1]. However, the reading of the pointer meter is mainly manual and some meters are in complex environments such as high altitude, high pressure and high radiation, so staff cannot take the reading easily, quickly and effectively. This has caused the problems of difficult reading, large reading error, large workload and poor timeliness [2]. Therefore, the automatic reading of pointer-type meters is of great importance for the development of intelligent industry [3]. With the rapid development of artificial intelligence, machine vision has become effective in attaining industrial images and video information [4]. Accordingly, the accuracy and efficiency of reading recognition in large-scale industrial practice have been enhanced thanks to the application of machine vision in industrial meter reading and other technologies [5].

The meter reading obtained by the computer is completely different from a manual reading. The computer can only achieve results based on its own observations, while individuals can adapt to the results that they see. Due to the

* Author to whom any correspondence should be addressed.

complexity and diversity of the natural environment, a meter image captured by an industrial camera may be inclined and rotated. This will result in a complex circumstance with significant problems for the computer to read the pointer readings from a meter image, and the solution to this problem is imminent [6].

Thus far, many people have put forward methods for the reading of pointer meters, which can be divided into three categories:

1.1. Methods based on feature matchings

Lai *et al* realized meter scale bar recognition based on a scale search and value inference algorithm, and further used the distance from the pointer to the adjacent scale bar to calculate the meter reading [7]. Hou *et al* used the contour features of edge detection and a template meter image for feature registration of the matched image, to obtain the perspective matrix between the two images, and recognized the correction of the meter [8]. Gang *et al* used the accelerated-KAZE algorithm to extract the feature points of the preprocessed image and the template image, then also applied the cosine similarity as the index of image registration for meter detection and positioning [9]. The method of feature registration involves a fixed meter template, so this method is lacking in universality.

1.2. Computer vision methods

Alegria and Serra detected the position of the pointer in a pointer meter and achieved number recognition in the digital meter, based on early stage computer vision technology [10]. Wang *et al* used a structured random forest edge detection algorithm and canny edge detection algorithm, further combined with Hough straight line detection to detect the pointer of the meter, and completed automatic meter reading recognition [5]. Wu *et al* accomplished the reading of a substation meter pointer based on digital image processing technology, and proposed an adaptive gamma image enhancement algorithm based on Retinex theory to finalize the details and colors of the image [6]. Yifan and Qi solved the pointer shadow issue by utilizing the binary threshold determination method based on symmetry, and proposed an improved random sample consistency algorithm to identify the pointer [3]. Based on the centrality of the scale line of the circular meter, Zhuo *et al* used Hough straight line detection to locate the scale line, and used the maximum probability criterion to locate the rotation center of the pointer by using the grid center of the intersection of all the scale lines [11]. Zhu *et al* fit the elliptical area of the meter panel based on particle swarm optimization, applied the straight line extraction method to fit the pointer straight line, and further used the span between the scale values to determine the maximum scale value and the minimum scale value, then lastly used the angle method to obtain the meter reading [12]. Yuan used image processing technology and the five-point ellipse fitting method to identify the pointer reading, and combined the distance between the pointer and the meter panel to reduce the reading error [13]. Xu and Xiong made full use of the gray-scale information of the image to locate the meter center based on the principle of energy minimization, by using the gray-scale image difference between the meter panel and the background image [14]. Liu recognized the pointer of the meter based on the motion characteristics of the gray-scale change rules of the image sequence, combined with the fuzzy c-means and fuzzy support vector machine unsupervised classification algorithms, and obtained the intersection center point of the scale value straight line as the rotation center of the pointer through Hough transformation. Finally, the angle method was used to obtain the pointer reading of the meter [15]. Based on the principle that the light reflected by images of different rotations of the pointer is different, Wang proposed the line scan method to detect the pointer of the meter [16].

1.3. Deep learning based methods

Zuo *et al* constructed a convolutional neural network (CNN) model based on region-CNN (RCNN) to classify the pointer meter while detecting the pointer of the meter, and used the angle method to take the reading of the meter [17]. Zhang *et al* classified the meter based on Faster-CNN, and then used image processing technology to locate the pointer to complete meter correction, pointer extraction, scale repair, and reading acquisition [18]. Lei *et al* classified multiple types of meters based on Mask-RCNN, and then performed digit recognition and pointer reading acquisition through the binary mask identified by Mask-RCNN [19]. Cai *et al* used virtual sample generation technology to generate a variety of meter samples, used the generated large number of samples to train the recognition model, and finally used Hough circle detection and other methods to take the meter readings [20]. Based on the YOLOv4 model, Zhang and Cao used the Canopy algorithm and K-means++ algorithm to replace the original K-means algorithm, and replaced path aggregation network with the feature pyramid network structure. They proposed a new model to detect the positioning meter, and compared the proposed method with Fast-RCNN, YOLOv4 and the improved YOLOv4 model [21]. Lin *et al* implemented an intelligent meter reading system based on the YOLOv3 model and RK3399 microcomputer [22]. Zhang *et al* located the different pointer areas in a water meter based on the improved YOLOv4 model, established the corresponding rectangular coordinate system for the pointer area to realize the pointer reading, used the combination of key point detection and pointer coordinate system positioning to identify the meter reading, and then compared it with Hough detection and other methods [23]. Zhou *et al* extracted the scale value position in the meter based on YOLOv3, used the five-point method to fit the scale value ellipse, used the relationship between the ellipse and the circle to carry out perspective correction of the meter, further used the scale position relationship to carry out the rotation correction of the meter, and finally used image processing technology to obtain the meter reading [24]. Wang *et al* located the meter panel area based on the Faster-RCNN target detection algorithm, enhanced the data set using the Poisson fusion method, and obtained readings through image processing methods such as Hough detection [25].

In the above studies, most of the studies did not correct the meter image when obtaining the meter pointer reading, but only the collected meter image was studied. Nevertheless, in real situations, the acquired images may have perspective transformation and rotation transformation. After the correction of the meter image, the accuracy of the pointer reading in the second stage will be improved qualitatively. Secondly, for the acquisition of meter readings, whether the distance method or the angle method is used, the scale value needs to be acquired. Nevertheless, the current method utilizes the color difference method, template matching method and key point detection method between the scale value and the meter panel, and lastly needs to use image processing technology to identify the scale value, which will have a certain impact on the timeliness in an actual application. The use of image processing technology should be minimized in the reading stage. Lastly, there will be accumulated errors from the meter panel positioning, image processing, scale acquisition, and straight line fitting to the final reading calculation, which will also lead to certain errors in the final reading results.

According to the above problems, in the research described in this paper, the problems of perspective correction, rotation correction and pointer reading recognition of circular pointer-type meters are solved for three types of circular pointer-type pressure gauges, namely 0–2.5 MPa, 0–10 MPa and 0–25 MPa. Obtaining information about the position of the scale values in the meter and the numerical information of the scale values is the basis for meter correction and pointer reading identification. Consequently, based on the YOLOv5s target detection model, this paper detects and identifies 14 scale values between 0 MPa and 25 MPa. The least square method is used to fit the elliptic curve equation of the scale value, and the perspective matrix from ellipse to circle is calculated by using the relationship between ellipse and circle. The center of the ellipse is used as the center of rotation of the pointer, so that the equation of the corrected scale value circle and the center of rotation of the pointer are the same circle center, making all the calculation processes in the same coordinate system. We use the minimum value and maximum value of the scale value to complete the rotation correction of the meter image, based on the horizontal coordinate axis of the image. The scale value coordinates detected by the target detection model are simultaneously using the correction matrix. For the corrected image, the morphological variation of the image is used to obtain the root region of the pointer, and the mathematical properties of the obtained connected region are used to determine the pointer linear equation and the pointer tip. The distance method is proposed to locate the direction of the pointer tip, and eventually the weighted angle method is used to obtain the pointer reading, so as to further eliminate the accumulated error in the reading recognition process.

The main contributions of this article can be summarized as follows:

(a) This paper uses a target detection network to obtain the scale values of the meter panel, to provide the necessary information for the subsequent correction and reading identification stages.
(b) This paper provides a perspective correction and rotation correction method based on the scale value of the meter panel, which completes the correction of the meter image and solves the problem that the actual captured meter image is skewed.
(c) In this paper, the center of the scale value circle is used as the center of rotation of the pointer, avoiding the problem that the center of rotation and the center of the scale value do not share the same point.
(d) This paper provides a weighted angle method with multiple scale values to determine the meter reading to improve the accuracy of meter reading.

The remainder of this paper is organized as follows:

Section 2 provides the relevant research ideas and algorithmic steps. Section 3 compares the differences between the proposed method and the traditional method and further provides a detailed analysis of the experimental results. Section 4 summarizes the contributions of this paper and the shortcomings of the method, and provides an outlook for future research.

2. Overview of meter correction methods

For the recognition of meter pointer readings, this paper is divided into two stages. First, the scale values on the meter panel are recognized according to the YOLOv5s target detection model, and the location information and numerical information of the scale values are obtained. Second, meter correction and pointer reading recognition are performed by using the scale value information. The whole process is shown in figure 1.

2.1. Meter panel scale detection and recognition based on YOLOv5s

In the traditional meter pointer reading recognition method, image processing technology is used to obtain the scale of the meter panel and the deep learning method is used to detect the scale position, which does not identify the scale value. As a result, it is necessary to re-identify the detected scale in the subsequent meter pointer reading recognition stage. The Yolov5s network has the advantages of fast image processing, detecting image scale value location and scale value information, small final training weight file, and the suitability for small devices. Therefore, this paper detects and identifies the scale values of the meter panel based on the YOLOv5s target detection model to provide the necessary information for subsequent meter correction and obtaining the pointer readings.

YOLOv5 is an advanced model in the YOLO family, where the model complexity increases in the order of YOLOv5s, YOLOv5m, YOLOv5l and YOLOv5x. This paper utilizes the smallest model in YOLOv5 to detect the scale information in the meter panel. YOLOv5s uses the original Mosaic data enhancement method to randomly scale, crop and arrange the training data. The adaptive anchor frame calculation method is embedded in the calculation, and the image filling method with small pixel value loss is used. In YOLOv5s, a cross stage

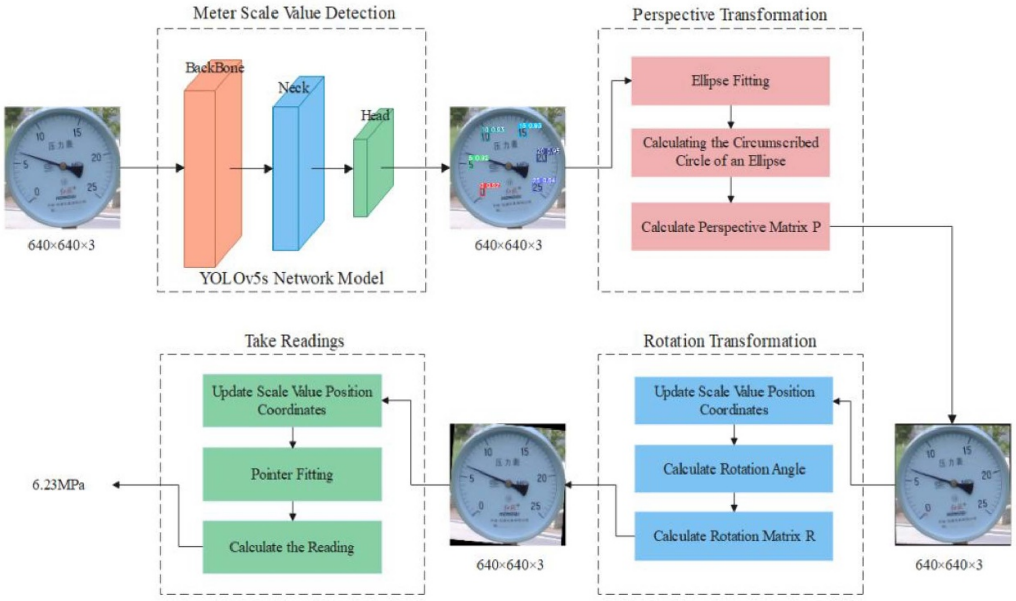

Figure 1. Overall flow chart of meter correction and pointer reading identification.

partial (CSP) structure different from that of YOLOv4 was used. The CSP1_X structure is applied in the BackBone network, while the CSP2_X structure is applied in Neck. The CIOU_Loss loss function is adopted in YOLOv5s. The BackBone is a feature perspective for acquiring an input image. The Neck is used for feature fusion of the different dimensions. The Head is used to generate the final location and category of the target. In this paper, the YOLOv5s target detection network is trained to detect 14 scale values in the meter panel. The detection results in this paper are illustrated in figure 2.

(a) (b) (c)

Figure 2. Meter scale value detection result chart based on YOLOv5s. (a) (0 – 2.5 MPa). (b) (0 – 10 MPa). (c) (0 – 25 MPa).

2.2. Meter correction

In everyday situations, the camera takes distorted pictures due to complex shooting environments, which will result in some deformation of the scale values, pointer positions and actual positions in the meter. In article [10], it is pointed out that the error of the calibrated meter image reading is lower than the range recognizable by the human eye. The correction of the pointer meter image directly affects the final reading of the meter [8]. By re-identifying the meter reading from the tilt-corrected meter image, the accuracy of the reading was significantly improved [24]. All of the above mentioned articles illustrate that the accuracy of meter readings can be improved after meter correction. In order to address the errors in meter readings due to skewed meter images, it is necessary to calibrate the meter images. The meter correction in this paper includes perspective correction and rotation correction, and the process is done based on the position of the scale value of the meter panel during the target detection phase.

2.2.1. Perspective correction. For the circular pointer-type meter, when the camera is perpendicular to the meter panel, the acquired image is the front view. At this time, the scale value of the meter panel is on the circle with the rotation center of the pointer as the center [10]. When the camera is shooting at a certain angle, the scale value of the meter panel will be distorted and located on the ellipse centered on the rotation center of the pointer. Based on the result that the circle turns into an ellipse after the meter panel is distorted, the inverse transformation can be carried out to obtain the elliptic equation where the meter panel scale is located. According to the relationship between the ellipse and the circle, the perspective matrix can be obtained, and finally the perspective of the meter panel scale value can be corrected. In this paper, the elliptic equation of the scale value position is fitted according to the scale value information extracted by YOLOv5s. The extension line of the long axis and the short axis of the ellipse is used to establish a perspective relationship with the intersection of the ellipse and the tangent circle of the ellipse to realize the perspective correction for the meter.

In image processing, ellipses are widely used to represent the distribution of spatial points. At present, the ellipse fitting methods commonly used include the five-point method, Hough transform method and least square method [26]. Because the number of key points detected in the target detection stage is unpredictable, and ellipse fitting is required according to the detected key points, this paper utilizes the

least square method to fit the ellipse equation where the correction value of the meter is located.

Equation (1) is the general equation of an ellipse:

$$Ax^2 + Bxy + Cy^2 + Dx + Ey + 1 = 0. \tag{1}$$

The least square method is used to fit the detected scale value coordinates of the meter. A rectangular coordinate system is established with the upper left corner of the image as the origin, which satisfies the right-hand rule; the right side of the origin is the positive x axis direction, and the lower side of the origin is the positive y axis direction. The process of fitting is to find the parameter groups (A,B,C,D,E) so that the error of all detected key points in equation (1) is the smallest even if equation (2) is the smallest:

$$f(A,B,C,D,E) = \sum_{i=1}^{N} \left(Ax_i^2 + Bx_iy_i + Cy_i^2 + Dx_i + Ey_i + 1\right), \tag{2}$$

where N represents the number of scale values detected and (x_i, y_i) represents the coordinates of the i key point detected. Figure 3 is an ellipse result diagram showing the position of the scale value fitted by the least square method.

According to the fitted ellipse equation, and further performs perspective transformation on the ellipse to convert the fitted ellipse into a perfect circle. Perspective transformation requires four sets of corresponding keys before and after transformation, and any three keys are not collinear. Consequently, it is necessary to find the set of key points before perspective transformation $\{S_1, S_2, S_3, S_4\}$ and the corresponding set of key points after perspective transformation $\{S_1', S_2', S_3', S_4'\}$.

The steps of computing the perspective transformation matrix are as follows:

(a) Linear equation for calculating the long and short axes.

The geometric center (x_c, y_c) of the ellipse can be obtained from equation (3):

$$\begin{cases} x_c = \frac{BE - 2CD}{4AC - B^2} \\ y_c = \frac{BD - 2AE}{4AC - B^2} \end{cases}. \tag{3}$$

The lengths of the short axis a and the long axis b of the ellipse are obtained from equation (4):

$$\begin{cases} a^2 = \frac{2\left(Ax_c^2 + Bx_cy_c + Cy_c^2 - 1\right)}{A + C + \sqrt{(A-C)^2 + B^2}} \\ b^2 = \frac{2\left(Ax_c^2 + Bx_cy_c + Cy_c^2 - 1\right)}{A + C - \sqrt{(A-C)^2 + B^2}} \end{cases}. \tag{4}$$

Calculate the horizontal inclination angle θ of the long axis of the ellipse with equation (5):

$$\theta = \begin{cases} 0, & B = 0, A < C; \\ \frac{1}{2}\pi, & B = 0, A > C; \\ \frac{1}{2}\arctan\frac{B}{A-C}, & B \neq 0, A < C; \\ \frac{1}{2}\pi + \frac{1}{2}\arctan\frac{B}{A-C}, & B \neq 0, A > C. \end{cases} \tag{5}$$

(a) (b) (c)

Figure 3. Ellipse fitting result of meter scale value position. (a) (0 – 2.5 MPa). (b) (0 – 10 MPa). (c) (0 – 25 MPa).

According to the horizontal angle of the long axis, the slope of the linear equation $k_b = \arctan\theta$ can be obtained. The slope of the linear equation of the short axis $k_a = -\frac{1}{k_b}$. Equations (6) and (7) respectively represent the linear equations of the long axis and the short axis of the ellipse:

$$y = k_b x + y_c - k_b x_c, \tag{6}$$

$$y = k_a x + y_c - k_a x_c. \tag{7}$$

(b) Calculate the intersection of the long and short axes with the ellipse and the circle, respectively.

The tangent equation of the ellipse is determined by the ellipse center (x_c, y_c) and the long axis b, as illustrated in equation (8):

$$(x - x_c)^2 + (y - y_c)^2 = b^2. \tag{8}$$

Then calculate the intersection point between the linear equations (6) and (7) of the long axis and the short axis and the elliptic equation (1), that is, the set of key points $\{S_1, S_2, S_3, S_4\}$ before perspective transformation. According to the linear equations (6) and (7) of the long axis and the short axis, calculate the intersection point with the elliptic tangent equation (8), that is, the set of key points $\{S_1', S_2', S_3', S_4'\}$ after perspective transformation. The intersection point set is illustrated in figure 4.

(c) Calculate perspective matrix based on the intersection set.

The complete form of perspective transformation is illustrated in equation (9):

$$\begin{bmatrix} x \\ y \\ w' \end{bmatrix} = P \begin{bmatrix} u \\ v \\ w \end{bmatrix} = \begin{bmatrix} a_{11} & a_{12} & a_{13} \\ a_{21} & a_{22} & a_{23} \\ a_{31} & a_{32} & a_{33} \end{bmatrix} \begin{bmatrix} u \\ v \\ w \end{bmatrix}, \tag{9}$$

where (u, v, w) is the two-dimensional homogeneous coordinate in the original image and (x, y, w') is the two-dimensional homogeneous coordinate after perspective transformation. Let $w = 1$, the two-dimensional plane coordinate (x', y') after perspective transformation is calculated using the following equation (10):

$$\begin{cases} x' = \frac{x}{w'} = \frac{a_{11}u + a_{12}v + a_{13}}{a_{31}u + a_{32}v + a_{33}} \\ y' = \frac{y}{w'} = \frac{a_{21}u + a_{22}v + a_{23}}{a_{31}u + a_{32}v + a_{33}} \end{cases}. \tag{10}$$

Figure 4. The result of the long and short axes of the ellipse where the scale value of the meter is located, and the intersection with the ellipse and the circle is also shown.

Substitute the four groups of key point coordinates $\{S_1, S_2, S_3, S_4\}$ and $\{S_1', S_2', S_3', S_4'\}$ before and after perspective transformation into equation (10) and let $a_{33} = 1$. Eight parameter values are obtained by solving the equation to obtain the perspective matrix P.

The perspective corrected image of the meter image is calculated according to the perspective matrix P. The perspective correction results of the meter images are shown in figure 5.

2.2.2. Rotation correction. Perspective transformation allows the method to obtain a full circle map of the dashboard scale values. However, if there is an angular rotation of the captured meter panel in the image, the subsequent implementation of the readout recognition technique can lead to some errors. In article [24], it is pointed out that the simultaneous implementation of meter image perspective correction and rotation correction is of great importance for meter reading recognition. Secondly, the rotation of the meter image causes the scale value to be shifted from the position of the scale value in the posed meter. In the right-angle coordinate system, the slope of different lines will be varied, and the angle method in this paper needs to rely on the slope of the line between the scale value and the center of rotation. In this situation, the same scale values will be distributed almost at the same position in the right-angle coordinate system in the corrected meter image, so the line with the center of rotation will be fixed, and the slope between the center of rotation and each scale value will also be fixed. Therefore, when using the angular method to obtain pointer readings, more accurate readings will be obtained.

In this paper, the rotation correction of the meter panel is identified by using the relative angle among the connecting line between the minimum and maximum scale values of the circular pointer-type meter with the horizontal coordinate axis, and the identification of the scale values is done in the scale value detection stage. The schematic diagram of rotation correction is shown in figure 6.

Figure 5. Comparison results of perspective correction of a meter scale value. (a) Original image. (b) Scale value perspective corrected image. (c) Results of the fusion of (a) and (b).

Figure 6. Schematic diagram of rotation correction.

The steps of rotation correction are as follows:

(a) Calculate the new scale value coordinates after perspective transformation.

Use equation (10) to calculate the minimum scale value coordinates (x_s, y_s) and the maximum scale value coordinates (x_e, y_e) after the perspective change of the image.

(b) Calculate the slope k_l of the straight line using the following equation (11):

$$k_l = \frac{y_s - y_e}{x_s - x_e}. \tag{11}$$

(c) Calculate the midpoint coordinates (x_{se}, y_{se}) of the minimum and maximum scale value coordinates

$$\begin{cases} x_{se} = \frac{x_s + x_e}{2} \\ y_{se} = \frac{y_s + y_e}{2} \end{cases}. \tag{12}$$

(d) Calculate the angle δ of the straight line with respect to the horizontal coordinate axis where the minimum and maximum scale values are located:

$$\delta = \arctan k_l. \tag{13}$$

(e) For the case where angle δ only rotates the connecting line of the minimum and maximum scale values to be parallel to the horizontal coordinate axis, when the connecting

line of the minimum and maximum scale values is above the center of the circle where the scale values are located, the meter panel is not horizontally rotated at this moment. Consequently, the rotation correction angle β is calculated using the following equation:

$$\beta = \begin{cases} 0°, & x_{se} = x_c, y_{se} < y_c; \\ 180°, & x_{se} = x_c, y_{se} > y_c; \\ -90°, & x_{se} > x_c, y_{se} = y_c; \\ 90°, & x_{se} < x_c, y_{se} = y_c; \\ \delta, & x_{se} > x_c, y_{se} > y_c; \\ \delta + 180°, & x_{se} < x_c, y_{se} < y_c; \\ -\delta + 180°, & x_{se} > x_c, y_{se} < y_c; \\ \delta, & x_{se} < x_c, y_{se} > y_c. \end{cases} . \quad (14)$$

(f) Calculate rotation matrix R

$$R = \begin{bmatrix} \cos\beta & -\sin\beta & 0 \\ \sin\beta & \cos\beta & 0 \\ 0 & 0 & 1 \end{bmatrix} . \quad (15)$$

(g) Use the following equation to calculate the coordinate point after rotation:

$$\begin{bmatrix} x'' \\ y'' \\ w'' \end{bmatrix} = R \begin{bmatrix} x' \\ y' \\ w' \end{bmatrix} , \quad (16)$$

where, (x', y') is the new coordinate point after perspective transformation, (x'', y'') is the coordinate point after rotation, and $w'' = w' = 1$. Figure 7 shows the results of the comparison before and after the rotation correction.

2.3. Pointer reading identification

Meter pointer reading recognition is the ultimate goal of all of these processes. Consequently, an effective reading recognition method will get high accuracy recognition results. For the identification of the pointer reading, the most important thing is to detect the position of the pointer [27]. For the detection of the pointer, there are common methods such as the region growth method, depth learning based detection method and Hough straight line detection method. In this paper, a method of pointer detection and determination of the direction of the needle tip is proposed, and the pointer detection is completed.

The pointer of the pressure gauge has the characteristics of a large pointer root and small needle tip, and there is a large color difference between the color of the pointer and the background color of the meter panel [28]. Secondly, a half-pointer detection method is used to improve the accuracy and speed of pointer extraction [29]. In this paper, the root region of the pointer in the corrected meter image is first segmented using an adaptive thresholding method or a manually set threshold. Second, the morphological method is used to remove the noise of the threshold segmentation results and extend the root region of the pointer. Finally, the center of the segmented pointer root is determined by using the joint region center of mass, and the linear equation of the pointer root is obtained by using the regional linear fitting approach. The principle explanation diagram is shown in figure 8.

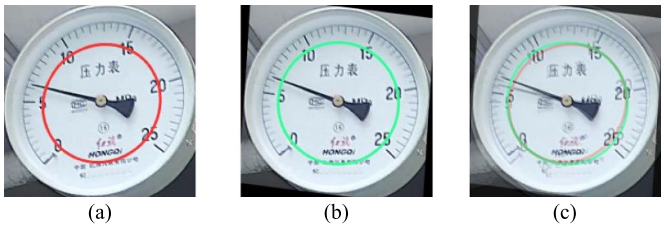

Figure 7. Results of rotation correction comparison chart. (a) Original image. (b) Rotation corrected image. (c) Results of the fusion of (a) and (b).

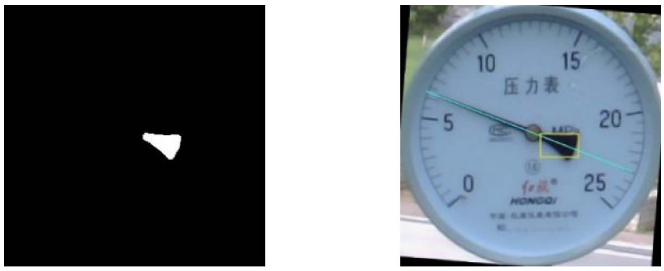

Figure 8. Interpretation diagram of fitting result of pointer linear equation. (a) Treatment results of pointer root. (b) Pointer straight line fitting and pointer root area frame fitting results.

Thereafter, the direction of the pointer needs to be determined. First, calculate the two intersection points P_a and P_b of the linear equation of the pointer and the circular equation of the key point fitting. Secondly, the O coordinate of the center point of the pointer root area is calculated according to the rectangle. Finally, the distance between the center point O and the intersection points P_a and P_b is calculated. Where the point $P_{\min}$ farthest from the point O is the point of the pointer, then the line connecting the center of the circle center (x_c, y_c) and $P_{\min}$ is the linear equation of the pointer. The process interpretation diagram is illustrated in figure 9.

Based on the angle method, this paper presents a weighted angle method to calculate the corrected meter reading. The angle method uses the line between the tip of the pointer and the center of rotation of the pointer, the line between the left and right scale values of the tip of the pointer and the center of rotation of the pointer respectively, and the angle in the middle of the three lines to determine the pointer reading. The interpretation diagram of the angle method is illustrated in figure 10. Utilize equation (17) to obtain the reading.

Where, α is the angle between the two scale values of the adjacent pointer relative to the center of the circle, and γ is the angle between the pointer straight line and the smaller scale value relative to the center of the circle.

Figure 9. Explanation diagram of pointer direction solution.

Figure 10. Interpretation diagram of the angle method.

The calculation equation of the pointer reading is as follows:

$$V = P_l + \frac{\gamma}{\alpha} \times (P_r - P_l), \tag{17}$$

where P_l is the smaller scale value adjacent to the pointer straight line, P_r is the larger scale value adjacent to the pointer straight line, and V is the final reading.

Nevertheless, there may be a cumulative error after the multiple processing of the previous image [30]. For this problem, this paper proposes a weighted angle method based on the angle method to reduce the cumulative error, so as to obtain an accurate meter pointer reading. Take the four scale values adjacent to the left and right of the pointer line, which are $P_{l2}, P_{l1}, P_{r1}, P_{r2}$, $P_{l2} < P_{l1} \leqslant P_{r1} < P_{r2}$, and the pointer line is located between P_{l1} and P_{r1}. Four groups of data are then formed, which are (P_{l1}, P_{r1}), (P_{l1}, P_{r2}), (P_{l2}, P_{r1}) and (P_{l2}, P_{r2}). According to the included angle between the scale value group and the center of the circle, each group is given different weights in order, with the largest angle and the smallest weight. The weights corresponding to the four groups of data are 0.4, 0.25, 0.25 and 0.1 respectively, and the weighted pointer reading is calculated as follows:

$$V = \sum_{i=1}^{4} w_i \left(P_{lk_1} + \frac{\gamma_i}{\alpha_i} \times (P_{rk_2} - P_{lk_1}) \right), \tag{18}$$

where, $W = \{0.4, 0.25, 0.25, 0.1\}$, $w_i \in W$, (γ_i, α_i) is the angle value of the i data pair, $k_1 = 1, 2$, $k_2 = 1, 2$.

3. Experiment

In this paper, fixed rotatable surveillance cameras from real places are used instead of special equipment dedicated to metered shooting. The captured real images are very realistic and high requirements are not demanded for image acquisition methods and equipment, making the method more generalizable. The acquired images include most of the backgrounds found in the real scenes, and for a better study targeting the meter readings, this paper uses a well segmented image of only the meter panel from the real scenes. The acquired images are various, with different tilt angles, rotation angles, light intensity and other cases. In this paper, three different types of meter images, four of each type for different environments, are selected to test the algorithm at different stages of the comparison experiments and to compare with the results of recent studies. Meter images with different illumination and different pointer shapes are also selected for comparison with existing pointer linear detection methods.

Image acquisition equipment: a fixed rotating camera is commonly used. The software and hardware environment for the experiments are: 64-bit Windows 10 operating system, 8G RAM, Intel(R) Core(TM) i7-7500U CPU@2.70 GHz, AMD Radeon(TM) 530 (2048 MB), Python 3.8.1, Pytorch 1.11.0 and OpenCV4.2.0.

3.1. Meter panel scale detection experiment based on YOLOv5s

As shown in figure 2, three main types of pressure gauges are used in this paper. There are 897 images in the experimental dataset, including 641 training sets, 128 validation sets and 128 test sets. The size of each image is 640 × 640 × 3. The detection target in each image includes all scale values in the dashboard. In this paper, we use the YOLOv5s target detection model with initial weights, which applies training weights from the coco128 dataset. We also set the AdamW as our gradient descent function, the batch size is set to 16 and epoch set to 200 as the base settings to train the scale value detection network.

The attenuation process of training times and average loss value is illustrated in figure 11. The iteration loss gradually decreases with the increase of training times. When it reaches epoch 160, the loss value gradually oscillates and the model gradually stabilizes.

As shown in figure 12, this paper uses a confusion matrix to describe the performance of the YOLOv5 scale value detection model. TP refers to the number of samples with positive class predicted as positive class by the model, and FP refers to the number of samples with negative class but predicted as positive class by the model. FN refers to the number of samples with positive true value but predicted as negative class by the model, and TN refers to the number of samples with negative true value predicted as negative class by the model.

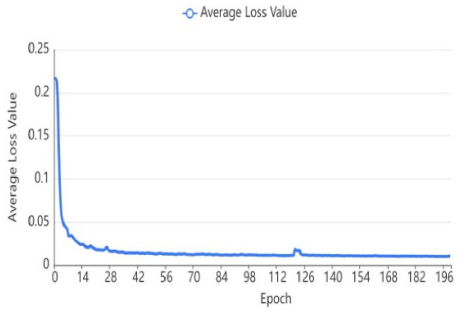

Figure 11. Attenuation process of training times and average loss value.

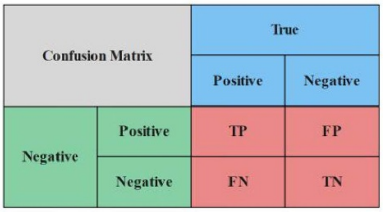

Figure 12. Confusion matrix interpretation diagram for binary classification.

The model trained in this paper, uses and trains the 128 test sets and gets an average value of 99.3% for mAP0.5. The average value of mAP0.95 reached 82.1%. As shown, the differentiation of categories is very clear in the results of the confusion matrix for the test set in figure 13, but there is also some easy confusion. For example, there may be a small confusion between the scale value 1 and the background, due to the presence of short straight lines similar to the number 1 in the background of the tick marks, numbers 10 and 15 in the dashboard, so the model will have some bias. There is also confusion between the scale values 5, 6 and the background, for a similar reason to the number 1, and the number 5 and the background are easily confused by the presence of 5 in other scale values, such as 0.5, 15 and 25. Second, the scale value 5 and scale value 6 are more similar in the meter, both in the rotation angle and vertical angle, so the scale value 5 and scale value 6 are more confused in the model prediction.

However, both the mAP value and the confusion ratio are high in the scale value detection model, so the model has an overfitting situation. The reason for this result is that the meter dials used in this paper occupy a larger position in the background image, and the scale value positions are basically distributed around the scale value rotation circle, and the scale value numbers vary greatly, etc. Therefore, the scale value detection model gets a better mAP value. Since meter correction and pointer reading identificationdepend on the accuracy of the model for scale value detection, the improvement of the recognition rate of the model for the scale value is ensured for the recognition of the later pointer readings.

In order to verify that the model can cope with various environments that may exist in the real world, this

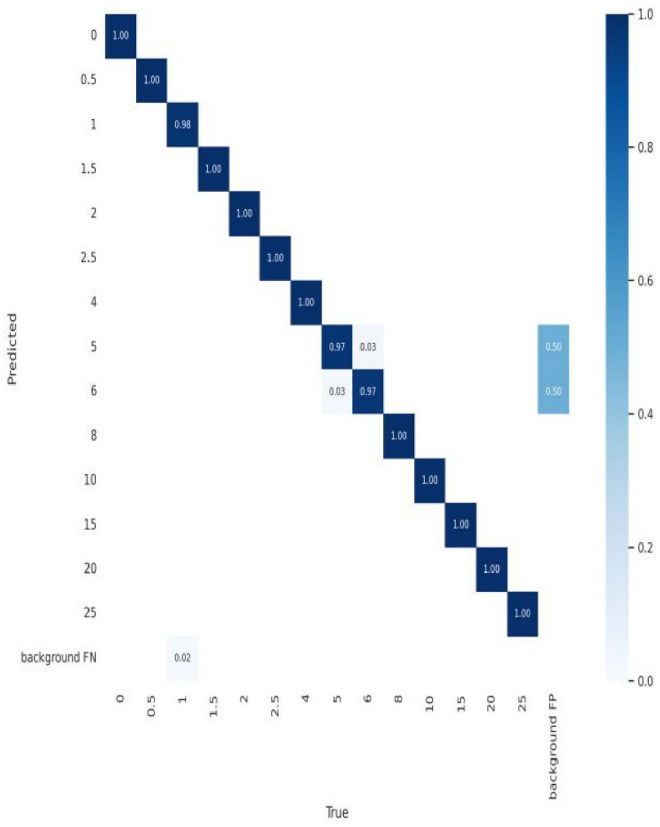

Figure 13. Visualization of the confusion matrix for the results of the test set.

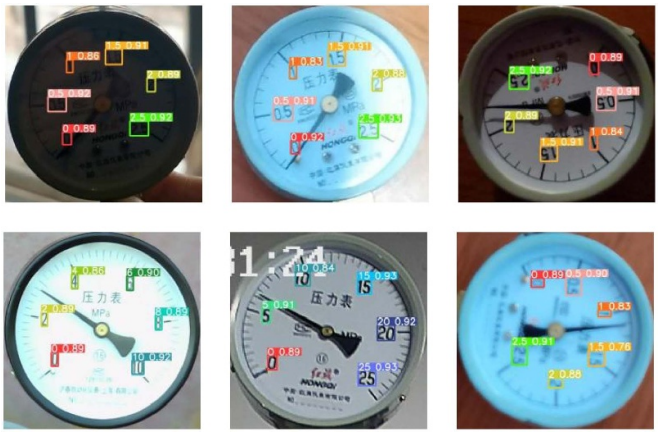

Figure 14. Meter image detection results in different environments.

paper tests the meters with various rotation angles, shooting angles and different illumination. The test results are illustrated in figure 14. The model established in this paper can solve the meter image under different situations in real environments and has good robustness. The weight file trained by the YOLOv5s model is only 14 Mb in size, which is suitable for small mobile devices in practical applications.

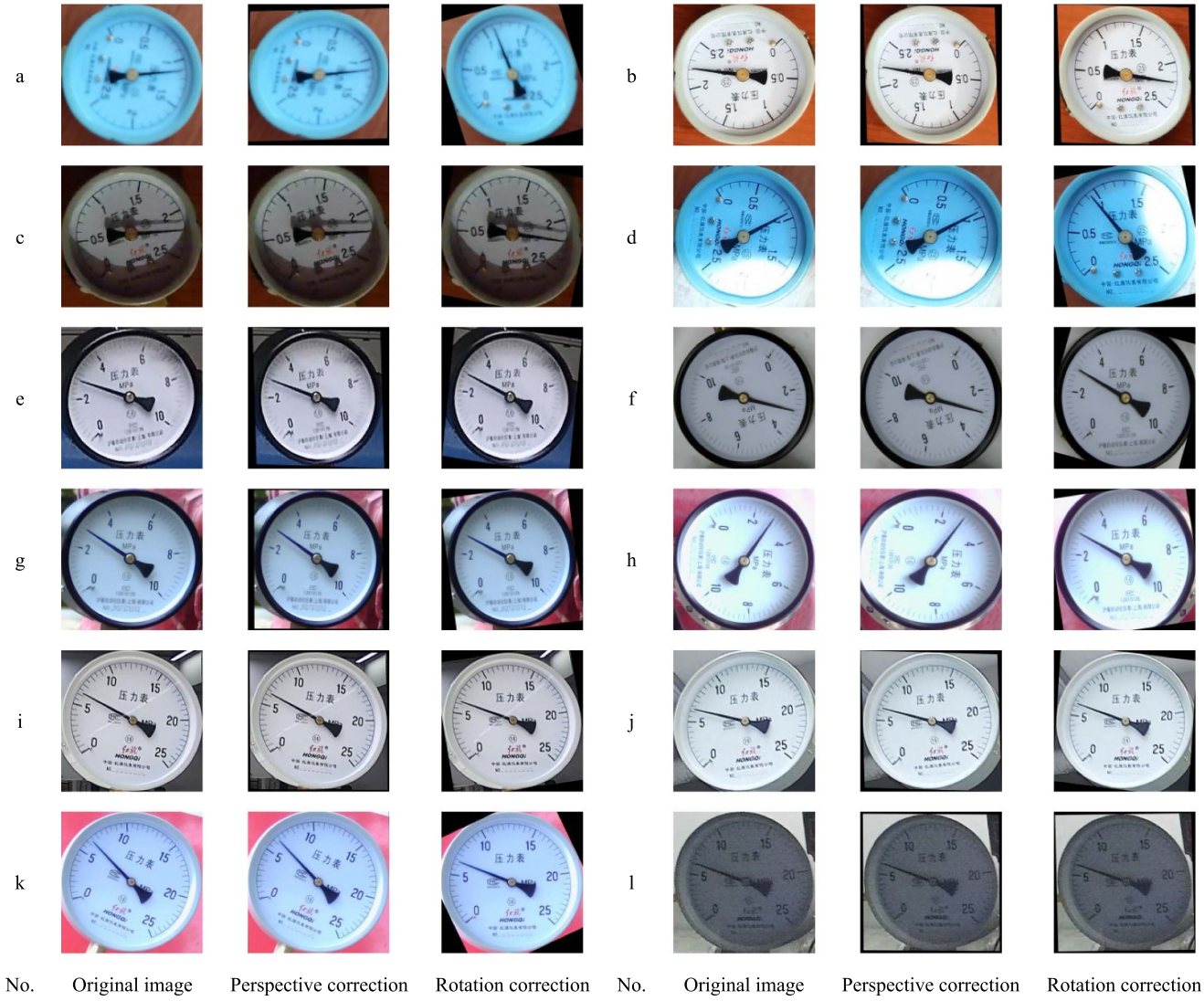

Figure 15. Comparison of meter correction results.

3.2. Meter correction experiment

The correction of the meter ensures the accuracy of pointer reading recognition. In this paper, perspective correction is realized based on the relationship between ellipse and circle, and the rotation correction of the meter is realized using the angle between the minimum scale value and the maximum scale value and the horizontal coordinate axis. The image correction results of real scenes are shown in figure 15.

The results of the correction angle for each figure compared with the manually measured rotation angle are shown in table 1. For the images in the experiments, the manually measured rotation angle was compared with the correction angle calculated by the algorithm in this paper. Comprehensive experiments were conducted for various rotation conditions. The algorithm in this paper produced results close to the manually measured rotation angles.

We next verify that the corrected meter images can improve the accuracy of meter reading. In this paper, the manual readings are compared with the results of readings with or without adding corrections and with or without using the weighted angle method proposed in this paper. The accuracy is measured by using the relational error δ and the reference error η. The calculation formula is shown in equation (19):

$$\begin{cases} \delta = \frac{|V_{\text{true}} - V_{\text{test}}|}{V_{\text{true}}} \times 100\% \\ \eta = \frac{|V_{\text{true}} - V_{\text{test}}|}{V_{\text{max}}} \times 100\% \end{cases}, \tag{19}$$

where, V_{true} represents the real value read manually, V_{test} represents the measured value read by the algorithm in this paper, and V_{max} represents the maximum scale value of the current meter to be tested.

Table 1. Comparison results of absolute values of meter rotation correction angle and artificial detection angle.

No.	Real (°)	Ours (°)	Error (°)
a	103.88	103.86	0.02
b	181.78	181.82	0.04
c	11.96	11.99	0.03
d	101.22	101.24	0.02
e	8.32	8.35	0.03
f	164.07	164.05	0.02
g	7.43	7.47	0.04
h	98.37	98.40	0.03
i	8.21	8.24	0.03
j	8.65	8.67	0.02
k	24.97	24.99	0.02
l	0.78	0.75	0.03
Avg.	—	—	0.028

In this paper, for the processing of readings from different meters, the following experiments were designed: reading the uncorrected meter image using the angle method (A), reading the meter image with only perspective correction using the angle method (P + A), reading the meter image after perspective correction and rotation correction using the angle method (P + R + A), reading the meter image after perspective correction and rotation correction using the weighted angle method (P + R + WA), the above process is used to read all the meter images in figure 15, and the meter reading results are shown in table 2.

The results in table 2 show that the average error of the uncorrected meter image readings obtained using the angle method is the largest, compared to the 50% reduction in the average error of the corrected meter image readings obtained using the angle method, which indicates that the corrected meter image improves the accuracy of the meter readings. The average error of the corrected meter image reading results using the weighted angle method is reduced by 75%, which shows that the algorithm in this paper does reduce the cumulative error of each process and improves the accuracy of the meter reading results. The reason for this result is that the corrected meter is on a positive circle for each scale value, so the angle between each scale is the same and therefore the reading error is reduced.

The average error of meter images read using the angle method that includes perspective correction and rotation correction is 50 percent lower than the error of readings that do not include rotation correction. This result illustrates that the addition of the rotation correction does improve the meter reading results. The reason for this result is that by adding the rotation correction, the scale values are fixed at the same position for each meter and only the position of the pointer changes in the image, so the accuracy of the readings will improve.

The reading error of the corrected meter image read using the weighted angle method is 50% lower than that of the corrected meter image read using the angle method, and this conclusion justifies the proposed weighted angle method in this paper. The reason for this result is that the traditional angle method only uses the maximum scale value and the minimum scale value to calculate the reading, but the spacing between these two scale values is large. The weighted angle method takes into account the four groups of scale values around the pointer and calculates the reading separately, and the most center weighting seeks to make each scale value produce a certain contribution to the reading.

Figure 16 more clearly depicts the meter reading results for the different algorithms in table 2. In figure 16, the error jumps produced by the different reading methods are larger for meters that represent a larger range. For example, the results for $i \sim l$, this is because for meters with larger scale values, each scale value cell expresses a larger range of data, so the reading results vary widely. However, their quoted errors are relatively small, indicating that errors have a small impact on such meters. As seen in figure 16, the relative error of $e \sim h$ is larger, which is due to the fact that in the 0 – 10 MPa type meters, the scale values are mostly single-digit, so the center of the individual scale values identified by the target detection will be shifted relative to the center of the two-digit scale values, so the error is larger than in the other two types of meters.

It can also be observed in figure 16 that the meter reading results without adding the rotation correction jump greatly, the reading results using the angle method for the corrected meter image are close to the manual reading, and the reading results using the weighted angle method for the corrected meter image are in the best agreement with the manual reading results. All of the above results illustrate the effectiveness of the algorithm in this paper. At the same time, reading the calibrated meter image with the traditional angle method also yields results close to the real reading, which also shows that the accuracy of the calibrated meter image on the reading results is improved to a certain extent.

Table 2. Comparison of the results of whether the meter adds correction with manual readings. Perspective correction (P). Rotation correction (R). Angle method (A). Weighted angle method (WA).

	Reading (MPa)					δ				η			
No.	Real	A	P + A	P + R + A	P + R + WA (Ours)	A	P + A	P + R + A	P + R + WA (Ours)	A	P + A	P + R + A	P + R + WA (Ours)
a	1.11	1.07	1.13	1.13	1.09	0.036	0.018	0.018	0.018	0.016	0.008	0.008	0.008
b	2.21	2.20	2.22	2.22	2.23	0.005	0.005	0.005	0.009	0.004	0.004	0.004	0.008
c	2.20	2.11	2.08	2.18	2.19	0.041	0.055	0.009	0.005	0.036	0.048	0.008	0.004
d	0.93	0.98	0.98	0.95	0.94	0.054	0.054	0.022	0.011	0.020	0.020	0.008	0.004
e	2.76	2.57	2.86	2.88	2.82	0.069	0.036	0.043	0.022	0.019	0.010	0.012	0.006
f	2.90	2.60	2.58	2.99	2.95	0.103	0.110	0.031	0.017	0.030	0.032	0.009	0.005
g	2.80	2.69	2.72	2.89	2.85	0.039	0.029	0.032	0.018	0.011	0.008	0.009	0.005
h	2.80	2.88	2.72	2.82	2.83	0.029	0.029	0.007	0.011	0.008	0.008	0.002	0.003
i	6.30	6.61	6.81	6.47	6.35	0.049	0.081	0.027	0.008	0.012	0.020	0.007	0.002
j	6.30	6.20	6.55	6.52	6.29	0.016	0.040	0.035	0.002	0.004	0.010	0.009	0.000
k	6.40	6.82	6.44	6.51	6.36	0.066	0.006	0.017	0.006	0.017	0.002	0.004	0.002
l	6.10	6.34	6.23	6.23	6.13	0.039	0.021	0.021	0.005	0.010	0.005	0.005	0.001
Avg.	—	—	—	—	—	0.045	0.040	0.022	0.011	0.016	0.015	0.007	0.004

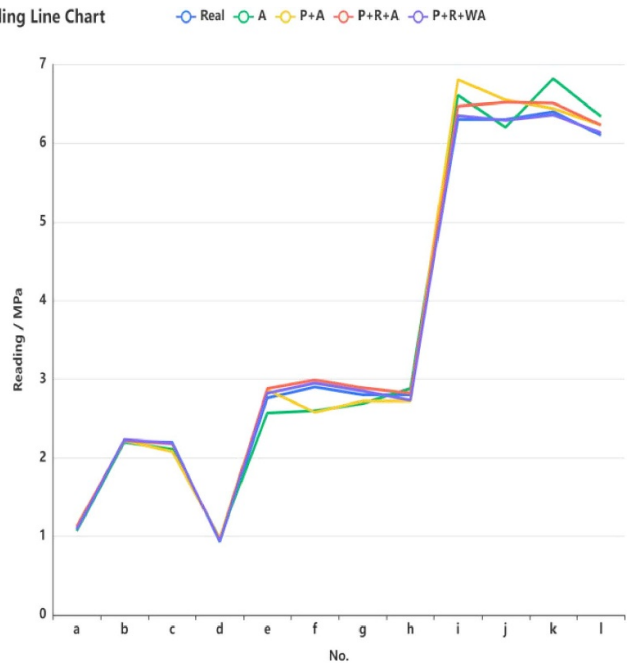

Figure 16. Table 2 folding line graph of the reading results.

3.3. Pointer detection comparison experiment

The pointer detection is the most critical step in the process of identifying the pointer reading of a circular pointer meter. In this paper, the pointer tip point is determined based on the root region of the pointer divided by the threshold. The pointer linear equation is determined from the line connecting the pointer tip point and the center of rotation.

Document [5, 11, 24] and others use Hough straight line detection to obtain the straight line equation of the left and right edges of the pointer, and determine the straight line equation of the pointer according to the intersection point of the straight line of the pointer edge at the pointer tip and the center of the meter. Zhou *et al* detected the first half section of the pointer tip using the YOLOv5 target detection network, and determined the pointer straight line equation according to the corner of the detection frame [29]. The experimental results of the pointer detection are shown in figure 17.

In figure 17, for the results of Hough straight line detection, the straight line detection will detect both the pointer's shadow and the pointer's edge straight line for meters with pointer shadow in the same threshold processing results, such as *h, i* and *j* in figure 17, leading to a large error in the final pointer straight line fitting results. In Hough detection, there may be multiple straight lines detected at the edges of the pointer, such as *a, b, c* and *g* in figure 17. After averaging the detected straight lines, the fitted pointer straight line equation will be biased towards the direction where most of the detected straight lines are. The method of using the marker detection network is to detect the position of the first half of the pointer. For extreme cases, as illustrated in *g, h, i*, and *j*, the detected pointer point is not on the corner of the rectangular box, which will have a large error in the fitting of the pointer linear equation. In this paper, the pointer straight line is first fitted using the root region of the pointer, which is used to determine the location of the pointer tip point. Finally, the pointer tip and the center of rotation of the pointer are used to determine the pointer line equation. This allows the pointer linear equation to always pass over the center of rotation, as a way to reduce the error in the pointer detection and final meter reading. As can be seen from figure 17, the pointer linear equation is well fitted in this paper for various complex environments.

3.4. Comparison experiments

In order to verify the rationality of the proposed algorithm, existing research methods are selected for comparison experiments in this paper. Yifan and Qi [3] used an improved RANSAC algorithm to detect the meter pointer, eliminate the pointer shadow, and then the 0 scale value and pointer angle to obtain the meter reading. Gao *et al* [31] designed a HOG/multiclass SVM digit classifier, detected the meter scale values, used the progressive probabilistic Hough transform (PPHT) algorithm to obtain the meter pointer, and finally used the angle method to obtain the reading of the car dashboard. Zhou *et al* [24] first used perspective correction and rotation correction for the meter panel, then used Hough linear detection to determine the pointer position, and finally used the angle method to determine the meter readings. In this paper, for

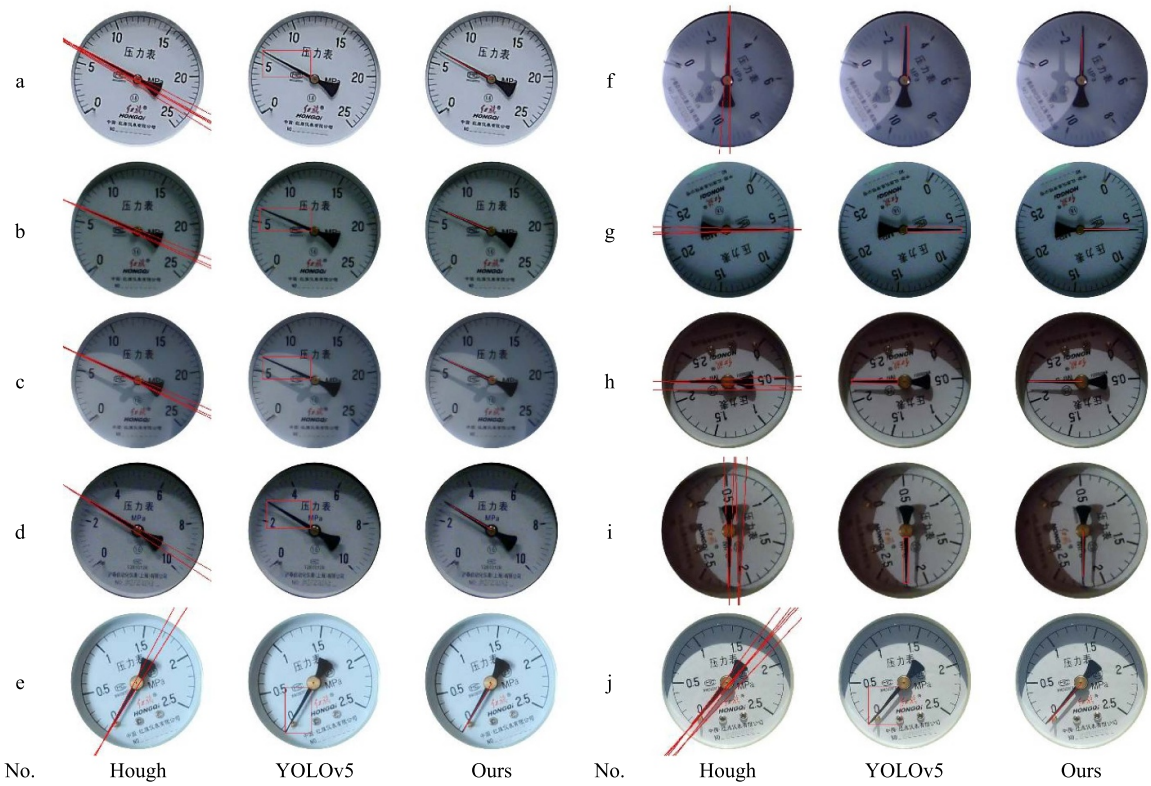

Figure 17. Comparison results of pointer detection.

all the meter images in figure 15, a comparison experiment was completed using the method described above. The results obtained by all algorithms were compared with manual readings, and the time consumed by all algorithms to complete a meter reading was also compared. The results of all comparisons are shown in table 3.

The comparison results in table 3 show that the average error of the reading results of the algorithm in this paper is lower than the average error of other algorithms. The meter images processed by Zhou *et al* and the algorithm in this paper are corrected meters, so the reading errors are lower than those of Ma *et al* from this result, thus it is known that the corrected meter image can reduce the error of the meter reading. The error of Zhou *et al* average meter reading results is higher than that of the algorithm proposed by Gao *et al*, because in the Gao *et al* method, the angle between the left and right adjacent scale values of the pointer is used, and the distance between the scale values is smaller, while Zhou *et al* uses the angle between the maximum and minimum scale values of the pointer, and the distance between the scale values is larger, so the error of the latter is greater. In contrast, the weighted angle method used in this paper combines the weighting of the reading results of several scale values in the vicinity of the pointer to obtain the meter readings, thus reducing the error due to the large distance of the referenced scale values. Its final reading result has a high degree of accuracy compared with several other algorithms, which confirms the effectiveness of the algorithm in this paper.

The duration of 1 m reading for the algorithm in this paper is 1.5 s, which meets the real-time meter reading requirement. Secondly, Gao *et al* uses the PPHT algorithm to eliminate the shadow background around the pointer in the meter. For *d, f, h* and *l*, there is less noise in the meter image results after using threshold segmentation and edge detection, so the readout time is shorter. Finally, the time required for each stage of this paper is shown in table 4.

Table 3. Comparison results with existing methods.

	Reading (MPa)					δ				η				Time (ms)			
No.	Real	[3]	[31]	[24]	Ours	[3]	[31]	[24]	Ours	[3]	[31]	[24]	Ours	[3]	[31]	[24]	Ours
a	1.11	1.07	1.15	1.13	1.09	0.036	0.036	0.018	0.018	0.016	0.016	0.008	0.008	771	2085	1377	1527
b	2.21	2.20	2.21	2.22	2.23	0.005	0.000	0.005	0.009	0.004	0.000	0.004	0.008	733	2073	1312	1486
c	2.20	2.11	2.12	2.16	2.19	0.041	0.036	0.018	0.005	0.036	0.032	0.016	0.004	790	2140	1475	1587
d	0.93	0.87	0.95	0.84	0.94	0.065	0.022	0.097	0.011	0.024	0.008	0.036	0.004	718	1451	1515	1584
e	2.76	2.57	2.83	2.72	2.82	0.069	0.025	0.014	0.022	0.019	0.007	0.004	0.006	954	2094	1376	1507
f	2.90	2.76	2.96	2.73	2.95	0.048	0.021	0.059	0.017	0.014	0.006	0.017	0.005	760	1611	1439	1566
g	2.80	2.62	2.88	2.71	2.85	0.064	0.029	0.032	0.018	0.018	0.008	0.009	0.005	870	2901	1419	1478
h	2.80	2.84	2.90	2.74	2.83	0.014	0.036	0.021	0.011	0.004	0.010	0.006	0.003	1137	1647	1401	1805
i	6.30	6.25	6.33	6.26	6.35	0.008	0.005	0.006	0.008	0.002	0.001	0.002	0.002	766	2905	1502	1599
j	6.30	6.27	6.34	6.11	6.29	0.005	0.006	0.030	0.002	0.001	0.002	0.008	0.000	749	2043	1318	1598
k	6.40	6.33	6.45	6.19	6.36	0.011	0.008	0.033	0.006	0.003	0.002	0.008	0.002	712	2052	1570	1535
l	6.10	6.41	6.35	6.01	6.13	0.051	0.041	0.015	0.005	0.012	0.010	0.004	0.001	708	1429	1385	1556
Avg.	—	—	—	—	—	0.035	0.022	0.029	0.011	0.013	0.008	0.010	0.004	806	2036	1424	1569

Table 4. Time consumption per processing step.

Process	Target detection	Perspective correction	Rotational correction	Pointer detection	Readings
Time (ms)	534	782	9	243	3

4. Conclusion

Through experimental comparison, the corrected pointer-type meter image provides a powerful guarantee for decreasing the error of meter pointer reading recognition, and it is of great significance for pointer reading recognition. For the shortcomings of traditional meter correction methods, this paper recommends a method based on CNN for meter image correction. Using the position information and value information of the scale value detected based on CNN, perspective correction and rotation correction of the meter are realized by using the least square method and the position of the minimum and maximum scale values. Based on the angle method, the weighted angle method is proposed to read the pointer readings, to solve the accumulated errors caused by multiple image transformations. This paper also uses the comparison method of adding different image processing stages to compare with manual readings to verify the effectiveness of the algorithm in this paper. Finally, this paper is compared with recent experimental results, and it is concluded that the reading results obtained from the corrected meter images have very small errors and are of practical value for applications in real environments.

The drawbacks of the algorithm in this paper are that the meter correction time is long and somewhat dependent on the meter characteristics during correction. Therefore, in future work, consideration can be given to reducing the reliance on meter characteristics during meter correction and meter readings.

Data availability statement

The data generated and/or analyzed during the current study are not publicly available for legal/ethical reasons but are available from the corresponding author on reasonable request.

Acknowledgment

This work was financially supported by China NSFC (Nos. 62192751 and 61425027).

ORCID iDs

Dongsheng Ji https://orcid.org/0000-0001-7955-365X
Wenbo Zhang https://orcid.org/0000-0003-4106-4038
Qianchuan Zhao https://orcid.org/0000-0002-7952-5621
Wen Yang https://orcid.org/0000-0001-8769-7370

References

[1] Zhang J, Liu Y, Yu J, Yang X, Yu X, Rodr J J and Gao H 2022 Automobile instrument detection using prior information and fuzzy sets *IEEE Trans. Ind. Electron.* **69** 13524–34
[2] Xu S, Hou C, Wang Z and Li B 2020 Pointer gauge adaptive reading method based on a double match *Meas. Sci. Technol.* **31** 115002
[3] Yifan M and Qi J 2020 Corrigendum: A robust and high-precision automatic reading algorithm of pointer meters based on machine vision (2019 *Meas. Sci. Technol.* 30 015401) *Meas. Sci. Technol.* **32** 019501
[4] Tan D, Chen L, Jiang C, Zhong W, Du W, Qian F and Mahalec V 2021 A circular target feature detection framework based on DCNN for industrial applications *IEEE Trans. Ind. Inform.* **17** 3303–13
[5] Wang C, Fang Y and Jia L (ed) 2018 The comparison of canny and structured forests edge detection application in precision identification of pointer instrument *2018 Chinese Control and Decision Conf. (CCDC)* (*9–11 June 2018*) pp 6361–5
[6] Wu X, Gao X and Gong J (ed) 2020 Intelligent instrument recognition scheme based on unattended substation inspection *2020 39th Chinese Control Conf. (CCC)* (*27–29 July 2020*) pp 6550–5
[7] Lai H, Kang Q, Pan L and Cui C (ed) 2019 A novel scale recognition method for pointer meters adapted to different types and shapes *2019 IEEE 15th Int. Conf. on Automation Science and Engineering (CASE)* (*22–26 August 2019*) pp 374–9
[8] Hou Z, Ouyang H and Hu X (ed) 2021 Tilt correction method of pointer instrument *China Automation Congress (CAC)* (*22–24 October 2021*) pp 608–12
[9] Gang P, Bing D, Chong C and Dingxin H 2022 Pointer-type instrument positioning method of intelligent inspection system for substation *J. Electron. Imaging* **31** 013001
[10] Alegria E C and Serra A C 2000 Automatic calibration of analog and digital measuring instruments using computer vision *IEEE Trans. Instrum. Meas.* **49** 94–99
[11] Zhuo H-B, Bai F-Z and Xu Y-X 2020 Machine vision detection of pointer features in images of analog meter displays *Metrol. Meas. Syst.* **27** 589–99
[12] Zhu J, Huang W, Chen W and Zhang X (ed) 2019 An ellipse fitting with PSO for automatic reading recognition of pointer instruments *2019 2nd Int. Conf. on Intelligent Autonomous Systems (ICOIAS)* (*28 February–2 March 2019*) pp 42–46
[13] Yuan F (ed) 2017 A method of correcting the pointer reading of deflection pointer instrument *2017 Chinese Automation Congress (CAC)* (*20–22 October 2017*) pp 5517–20
[14] Xu H and Xiong A (eds) 2019 Research on machine vision-based reading method for pointer meters *2019 Chinese Control Conf. (CCC)* (*27–30 July 2019*) pp 7544–9
[15] Liu H (ed) 2020 A novel vision based pointer instrument reading algorithm *2020 IEEE Int. Conf. on Artificial Intelligence and Information Systems (ICAIIS)* (*20–22 March 2020*) pp 661–4
[16] Wang Q 2022 Analog instrument pointer monitoring and parameter estimation via line scan vision *Energy Rep.* **8** 13076–82
[17] Zuo L, He P, Zhang C and Zhang Z 2020 A robust approach to reading recognition of pointer meters based on improved mask-RCNN *Neurocomputing* **388** 90–101
[18] Zhang X, Dang X, Lv Q and Liu S (eds) 2020 A pointer meter recognition algorithm based on deep learning *2020 3rd Int. Conf. on Advanced Electronic Materials, Computers and*

Software Engineering (AEMCSE) (*24–26 April 2020*) pp 283–7
[19] Lei L, Zhang H and Li X (eds) 2021 Research and application of instrument reading recognition algorithm based on deep learning *2021 3rd Int. Conf. on Artificial Intelligence and Advanced Manufacture (AIAM)* (*23–25 October 2021*) pp 535–9
[20] Cai W, Ma B, Zhang L and Han Y 2020 A pointer meter recognition method based on virtual sample generation technology *Measurement* **163** 107962
[21] Zhang Y and Cao N (eds) 2021 Research on instrument position detection method based on YOLOV4 *2021 Int. Conf. on Wireless Communications and Smart Grid (ICWCSG)* (*13–15 August 2021*) pp 554–60
[22] Lin Y, Zhong Q and Sun H 2020 A pointer type instrument intelligent reading system design based on convolutional neural networks *Front. Phys.* **8** 618917
[23] Zhang Q, Bao X, Wu B, Tu X, Jin Y, Luo Y and Zhang N 2021 Water meter pointer reading recognition method based on target-key point detection *Flow Meas. Instrum.* **81** 102012
[24] Zhou D, Yang Y, Zhu J and Wang K 2020 Tilt correction method of pointer meter based on deep learning *J. Comput.-Aided Des. Comput. Graph.* **32** 1976–84
[25] Wang L, Wang P, Wu L, Xu L, Huang P and Kang Z 2021 Computer vision based automatic recognition of pointer instruments: data set optimization and reading *Entropy* **23** 272
[26] Hu C, Wang G, Ho K C and Liang J 2021 Robust ellipse fitting with Laplacian kernel based maximum correntropy criterion *IEEE Trans. Image Process.* **30** 3127–41
[27] Zhang J, Liu Y, Li Y and Yu J 2022 A unified framework for automobile instrument detection system *IEEE Trans. Instrum. Meas.* **71** 1–11
[28] Hsiao F Y, Chang F-Y, Vida P, Kuo B C and Chen P-C 2022 Reading detection of needle-type instrument in a noisy environment using computer vision-based algorithms *Multimedia Tools Appl.* 1–34
[29] Zhou D, Yang Y, Zhu J and Wang K 2022 Intelligent reading recognition method of a pointer meter based on deep learning in a real environment *Meas. Sci. Technol.* **33** 055021
[30] Huo F, Li A, Ren W, Wang D and Yu T 2022 New identification method of linear pointer instrument *Multimedia Tools Appl.* 1–24
[31] Gao H, Yi M, Yu J, Li J and Yu X 2019 Character segmentation-based coarse-fine approach for automobile dashboard detection *IEEE Trans. Ind. Inform.* **15** 5413–24